Efficient generation of 1.9W yellow light by cascaded frequency doubling of a distributed Bragg reflector tapered diode

Hansen, Anders Kragh; Christensen, Mathias; Noordegraaf, Danny; Heist, P; Papastathopoulos, E; Loyo-Maldonado, V; Jensen, Ole Bjarlin; Skovgaard, Peter M. W.

Published in:
Applied Optics

Link to article, DOI:
10.1364/AO.55.009270

Publication date:
2016

Document Version
Peer reviewed version

Citation (APA):
Hansen, A. K., Christensen, M., Noordegraaf, D., Heist, P., Papastathopoulos, E., Loyo-Maldonado, V., Jensen, O. B., & Skovgaard, P. M. W. (2016). Efficient generation of 1.9W yellow light by cascaded frequency doubling of a distributed Bragg reflector tapered diode. *Applied Optics*, *55*(32), 9270-9274. https://doi.org/10.1364/AO.55.009270

Efficient Generation of 1.9 W Yellow Light by Cascaded Frequency Doubling of a DBR Tapered Diode

A. K. HANSEN[1,2], M. CHRISTENSEN[1,2,*], D. NOORDEGRAAF[1], P. HEIST[3], E. PAPASTATHOPOULOS[3], V. LOYO-MALDONADO[3], O. B. JENSEN[2], P. M. W. SKOVGAARD[1]

[1]*Norlase ApS, Risø Campus, Frederiksborgvej 399, 4000 Roskilde, Denmark*
[2]*Department of Photonics Engineering, Technical University of Denmark, 4000 Roskilde, Denmark*
[3]*JENOPTIK | Healthcare & Industry, JENOPTIK Laser GmbH, Göschwitzer Straße 29, 07745 Jena, Germany*
**Corresponding author: mac@norlase.com*

Received XX Month XXXX; revised XX Month, XXXX; accepted XX Month XXXX; posted XX Month XXXX (Doc. ID XXXXX); published XX Month XXXX

Watt level yellow emitting lasers are interesting for medical applications, due to high hemoglobin absorption, and for efficient detection of certain fluorophores. In this paper we demonstrate a compact and robust diode based laser system in the yellow spectral range. The system generates 1.9 W of single frequency light at 562.4 nm, by cascaded single pass frequency doubling of the 1124.8 nm emission from a distributed Bragg reflector (DBR) tapered laser diode. The absence of a free space cavity makes the system stable over a base-plate temperature range of 30K. At the same time the use of a laser diode enables modulation of the pump wavelength by controlling the drive current. This is utilized to achieve a power modulation depth of >90% for the second harmonic light, with a rise time <40 µs.

OCIS codes: *(140.3515) Lasers, frequency doubled; (140.3480) Lasers, diode pumped; (140.7300) Visible lasers.*

http://dx.doi.org/10.1364/AO.99.099999

1. Introduction

For decades, lasers in the green spectral region have been dominated by a wavelength of 532 nm due to its ease of access through frequency doubling of the 1064 nm emission from Nd:YAG crystals. For just as long there has been an interest in moving into the yellow or even orange spectral region, where there is a decrease in tissue scattering and melanin absorption[1]. Within flow cytometry, yellow emitting lasers can give access to previously unavailable fluorophores[2], and 561 nm lasers in particular have demonstrated an increase in the sensitivity of the detection of certain fluorophores[3]. The yellow-orange spectral region has also attracted attention within biomedical optics for photocoagulation[4], imaging[5, 6] and cancer treatment[7].

Today, yellow emitting lasers are produced using a range of technologies. Non-linear frequency converted diode pumped solid state (DPSS) lasers have produced powers greater than 1 watt at several wavelengths in the yellow-orange spectral range[8–10]. Unfortunately, they have a relatively low optical conversion efficiency (~10%), and therefore cannot run without water cooling. DPSS lasers emitting directly in the visible spectral range are possible using different Pr^{3+}, Sm^{3+}, Dy^{3+} and Tb^{3+} doped crystal host materials[11]. At 607 nm an output power of up to 1.8 W has been demonstrated when the laser was pumped with a frequency doubled optically pumped semiconductor (OPS) laser[12]. In Tb^{3+} doped fluorides up to approximately 100 mW has been demonstrated at around 585 nm[13]. Direct diode pumping has, however, resulted in significantly lower efficiency[11]. A significantly higher continuous wave (CW) power of 20 W has been demonstrated using OPS lasers[14]. However, these lasers suffer from the same drawbacks as the DPSS lasers. Another option is fiber lasers, but these tend to be either low power[15], pulsed[16, 17] or very complex[18] systems. Furthermore, a diamond based Raman laser have been demonstrated to emit pulsed light at 573 nm with a high conversion efficiency of 84% of the incident Q-switched laser light at 532 nm [19]. However, the need for pumping by a Q-switched laser limits the usability of such an approach.

For many applications, the ideal light source would be a laser diode due to its very small size, high efficiency and low cost. Recently, demonstration of laser operation in the yellow spectral range has been demonstrated in BeZnCdSe and InAlGaP devices with an output power of a few mW [20, 21]. However, laser diodes in the yellow-orange spectrum with watt-level output powers have so far eluded researchers. In the near infrared (NIR), on the other hand, tapered laser diodes are becoming commercially available. These laser diodes combine single frequency operation with output powers up to 8 W at 1120 nm[22]. Similar laser diodes with even longer wavelengths are also currently being developed[23]. These tapered laser diodes have been used to generate 550 mW at 561 nm using a planar waveguide in a non-linear crystal[24]. Waveguides in non-linear crystals enable high conversion efficiency[25], but suffer from power loss due to low coupling efficiency, scattering losses and decreased efficiency at high powers due to localized thermal effects[26]. To our knowledge the highest power achieved by frequency doubling the emission of a laser diode using waveguides in non-linear crystals are 860 mW for a channel waveguide[27] and 1.07 W for a planar waveguide[28].

In this paper we present a 1.9 W single frequency laser system at 562.4 nm, by single pass cascaded frequency doubling of the emission of a tapered laser diode. Cascaded frequency doubling is highly efficient, with second harmonic (SH) output powers even exceeding the sum of the SH powers achievable from each crystal individually. For a thorough description of the concept see [29]. Furthermore, we show that the simplicity of our system leads to a high thermal stability, thereby removing the need for water cooling. Combined with the small footprint of just 183 x 114 x 50 mm^3, this makes the laser system ideal for integration in larger systems.

2. Setup and Results

The experimental setup used for generating 562.4 nm light by direct frequency doubling of the emission of a 1124.8 nm laser diode is shown in Fig. 1. The laser diode is a tapered laser diode similar to the ones described in [22]. It is a monolithic device consisting of two sections: a ridge waveguide (RW) with a distributed Bragg reflector (DBR), and a tapered amplifier (TA). The chip is mounted with the epitaxial side up and the RW and TA sections are given separate contacts to allow for individual control of the currents. The laser diode emits a high power near-diffraction limited beam with 74% of the power in a Gaussian-like central lobe, and exhibits single-frequency operation. Due to the astigmatic output of tapered laser diodes two collimation lenses are used for correction. First the fast axis (vertical) is collimated using an aspheric lens (L_1, f = 2 mm). This lens refocuses the slow axis (horizontal), which is then collimated using a cylindrical lens (L_2, f = 5.8 mm). The beam is passed through an optical isolator (OI) to protect the laser diode from optical feedback. Mirrors M_1 and M_2 are plane mirrors used to steer the beam through the first non-linear crystal, while lens L_3 (f = 45 mm) focuses the beam to a waist diameter of ~85 µm, measured as $1/e^2$. Both the fundamental beam and the SH beam generated within the crystal are re-collimated using a concave mirror (M_3, R = 100mm) and passed through a dispersive plate (3 mm thick BK7) to optimize the phase offset between the two wavelengths, as described in [29]. The concave mirror M_4, which is identical to M_3, refocuses both beams into the second non-linear crystal, after which the fundamental beam is dumped and the second harmonic beam collimated. Both non-linear crystals are magnesium-oxide doped periodically poled lithium niobate (PPLN) with a poling period of 8.17 µm and a length of 40 mm. The length of the crystal was chosen based on previous results [29]. All lenses and crystals are AR coated for the relevant wavelengths and the mirrors are HR coated. The dispersive plate is placed at Brewster's angle to minimize reflections. The components are mounted on a baseplate and enclosed with a lid, giving the laser system a total size of 183 x 114 x 50 mm^3.

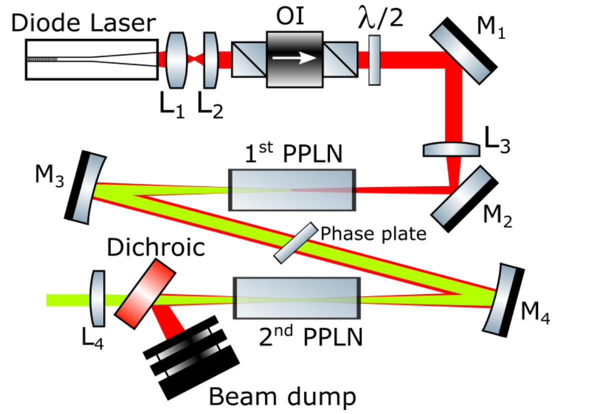

Fig. 1. Sketch of the experimental setup for cascaded frequency doubling.

The NIR power after the isolator is approximately 5.0 W with the laser diode operating at 300 mA on the ridge waveguide section, 10 A on the tapered amplifier and at a temperature of 20°C. Under these operating conditions, the wavelength of the laser diode is 1124.8 nm. With a NIR power of 5.0 W, 714 mW of second harmonic light is generated in the first crystal alone, at a crystal temperature of 77.8°C. Similarly, 857 mW is generated in the second crystal at 79.4°C. In both cases the measurement is performed by detuning one crystal 20°C from phase matching and measuring after the collimation lens (L_4). The non-linear conversion efficiency of the two crystals was measured to be approximately the same. The difference in power is due to differences in the beam paths through the crystals. With both crystals phase matched, the cascaded second harmonic power is 1.80 W, corresponding to 15 % more than the sum of the powers achievable by the crystals individually. When the currents through the laser diode are increased to 350 mA and 10.5 A, the NIR power after the isolator increases to 5.8 W, resulting in 1.93 W of second harmonic light. The lower conversion efficiency is due to a degradation of the beam quality at higher powers. At these operation conditions the total power consumption of the laser head, including heating of the crystals and cooling of the laser diode, is 30 W, yielding an electro-optical conversion efficiency of 6.4%.

The spectrum of the second harmonic emission was recorded using an optical spectrum analyzer (OSA) and is shown in Fig. 2. The figure shows that the laser system exhibits single frequency operation with a linewidth of less than 3 pm.

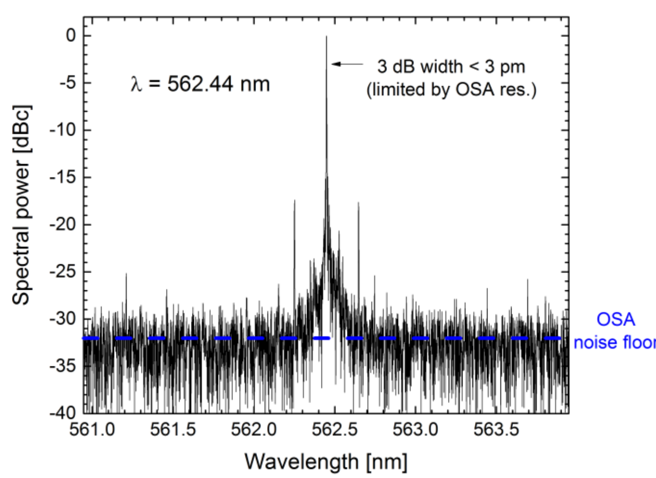

Fig. 2. Spectrum of the second harmonic light. The sidemodes seen at -18 dB are artifacts from the spectrum analyzer.

The M^2 of the 562.4 nm light was measured to be 1.32 in the horizontal axis and 1.37 in the vertical axis, see Fig. 3. The measurement was performed with a Spiricon M^2-200s beam profiler from Ophir Photonics.

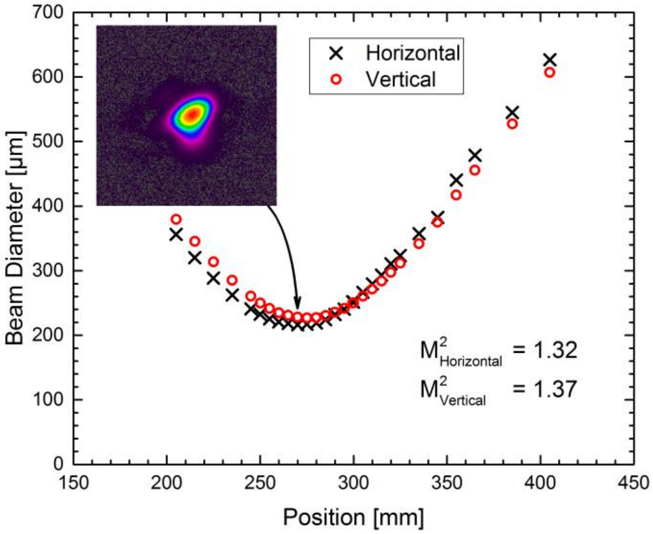

Fig. 3. M^2 measurement of the second harmonic output. The position on the x-axis is the distance to the focusing lens (f = 300 mm) and the beam diameter is the second moment diameter. The insert is an image of the beam in the point indicated by the arrow.

The turn-on behavior of the laser system was also investigated and even though the crystals were operated at temperatures just below 80°C the laser system could be turned on from cold in just 60s. This is illustrated in Fig. 4 which shows the output power of the laser system together with the temperature deviation of the laser diode and the two crystals from the set-point values. The figure shows that heating of the crystals is the main limiting factor, it is therefore expected that the 60s can be significantly reduced with more sophisticated thermal management.

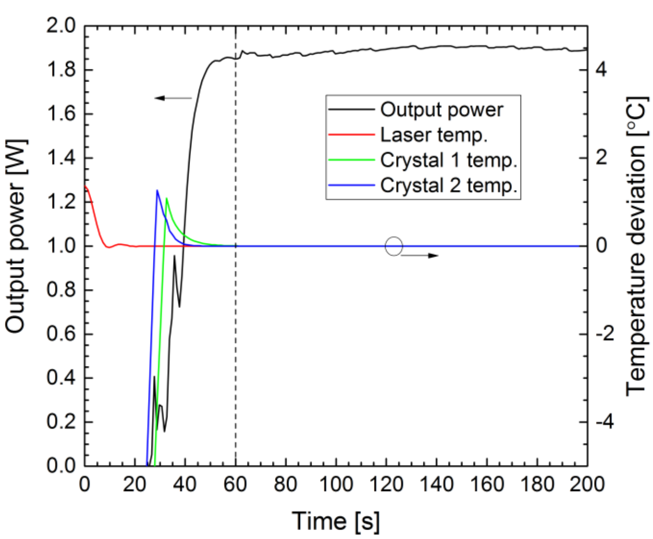

Fig. 4. Measurement of the laser system parameters during a start-up procedure. Both measurements are performed with the laser diode operating at 20°C, 350 mA ridge current and 10.5 A tapered current.

One of the advantages of using a single pass, rather than an external cavity system, is increased stability towards external perturbations. Although, the laser system is mounted on a water cooled plate, the system can be mounted on a forced-air cooled base plate because of its high temperature stability. This is illustrated in Fig. 5 where the water temperature was changed, leading to a change in the case temperature. For this test no active stabilization of the power was performed, but even so the attainable power output of the laser system remained above 1.7 W over a 30°C temperature span.

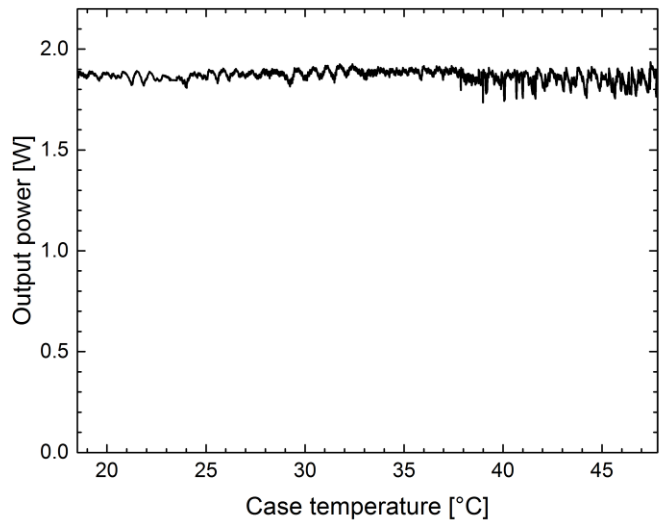

Fig. 5. Power output of the laser system as a function of case temperature. The laser system was operated at optimal phase matching. The temperatures of the crystals and the laser diode were stabilized, but there was no active stabilization of the power using a feedback loop. The test was performed over 100 minutes.

In another test, the long term power stability of the laser system was monitored while the output power was actively stabilized using feedback from a photodiode measuring the second harmonic power. The output was stabilized using the phase matching conditions of the laser and crystals, the result of which is shown in Fig. 6. For this test the case temperature had reached equilibrium. The standard deviation of the output power over these 250 hours was 0.5%.

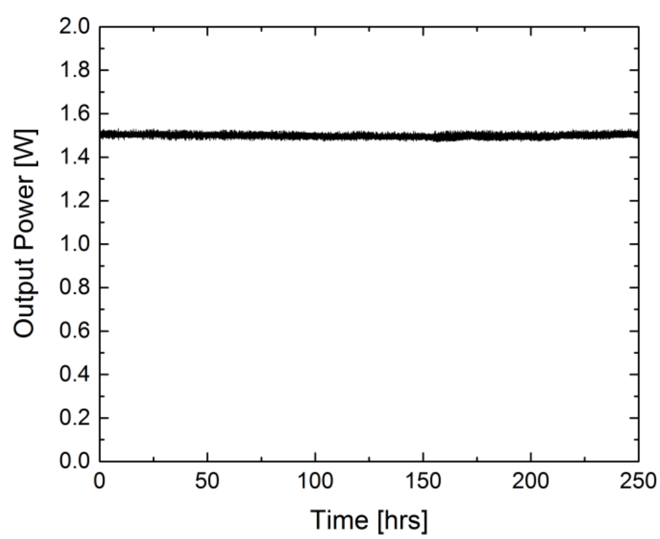

Fig. 6. Output power stability measured over 250 hours with active stabilization. Here the case temperature is constant.

Modulation frequencies of up to about 50 Hz are of interest within medical laser treatment. Here, systems based on laser diodes have an advantage due to the ability to modulate the second harmonic output power by modulating the current to the laser diode. In principle this can be done by gain-switching; i.e. turning the laser diode on and off. But in practice this leads to large thermal fluctuations of the laser diode chip, which in turn makes the wavelength, and therefore the second harmonic power, unstable. Alternatively, the wavelength can be modulated using its dependence on the injection current to the ridge section, thereby alternating between being close to, and being far from the phase matching condition of the nonlinear crystals. We used this approach to generate square second harmonic pulses with repetition rates ranging from 0.5 Hz to 50 Hz, the results at these two frequencies are shown in Fig. 7 and 8. The peak to peak modulation of the ridge current is 55 mA, which in CW operation corresponds to a wavelength shift of 37 pm. The theoretical full width at half maximum wavelength acceptance bandwidth of the cascade is 34 pm, assuming plane waves. The crystal temperatures remain unchanged from the CW case.

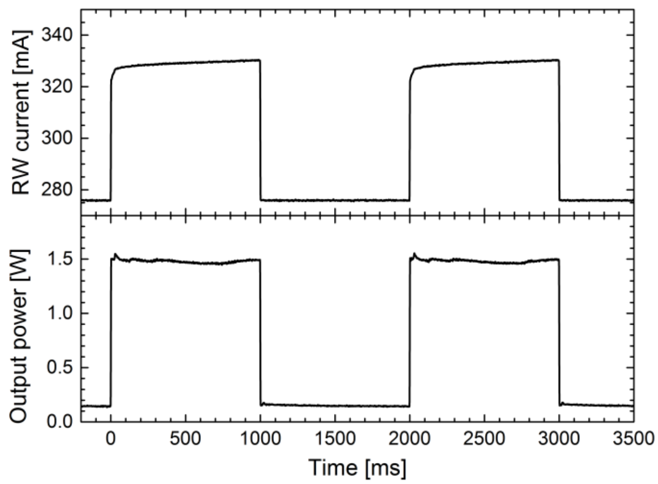

Fig. 7. 0.5 Hz modulation of the second harmonic light by adjusting the wavelength through the ridge waveguide current.

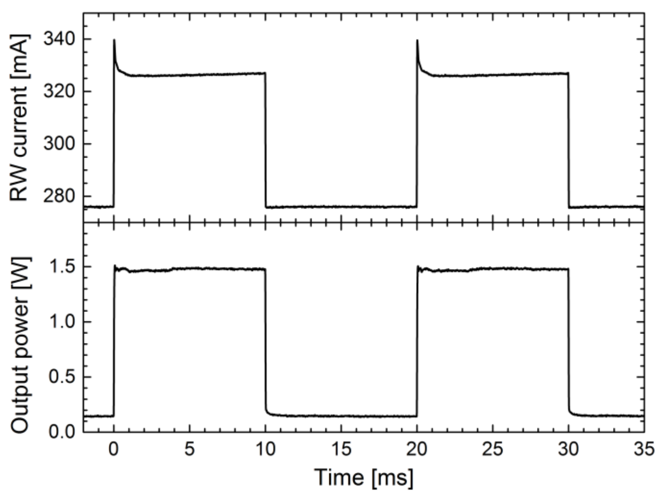

Fig. 8. 50 Hz modulation of the second harmonic light by adjusting the wavelength through the ridge waveguide current.

In the cases shown here the modulation was not to maximum power, but to the flank of the phase matching curve. Modulating only up to a point on the flank of the phase matching curve shows the wavelength stability throughout the pulse more clearly than when modulating to the phase matching peak. This is because the wavelength derivative of the second harmonic power, dP/dλ, is zero on the peak. Nevertheless, the on state of the pulse was very stable, which indicates that the ridge waveguide current is a good control for the wavelength. As shown in Fig. 7 and 8 a modulation depth >90% was achieved. Due to a small wavelength drift throughout the pulse, a tailored waveform was used to obtain square second harmonic pulses. The current through the ridge waveguide is therefore shown in the top parts of Fig. 7 and 8. One could in principle perform a deeper modulation on the current and achieve higher modulation depth. However, the mode hops of the laser diode were not well defined and therefore the laser has to be operated within one mode.

To estimate the rise and fall time of the pulse a zoom in on the first pulse from Fig. 8 is shown in Fig. 9. Here it can be seen that the rise and fall of the pulse is very regular, and the time it takes for the power to rise from 10 % to 90 % of the "on" state, or vice versa, is below 50 µs. This is mainly limited by the power supply which has a similar rise/fall time. The laser diode is expected to respond on a significantly faster time scale and with faster electronics it should be possible to achieve modulation above 10 kHz. This could be useful for medical laser treatment where micro-pulsing has been of interest. This is due to a more comfortable treatment without compromising the outcome of the treatment [30].

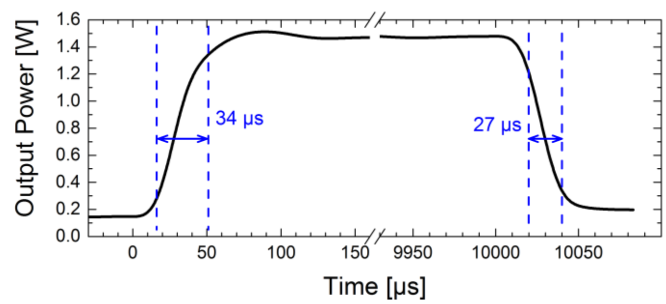

Fig. 9. 10% / 90% rise and fall time of the second harmonic power. The curves are a zoom of the rise and fall of the first pulse in the 50 Hz modulation (Fig. 8). Both the 10% and 90% levels are marked with vertical dashed lines.

A modulation depth of 100% could be achieved with a shutter or acousto-optic modulator. However, this would increase the size and cost of the laser. Our technique on the other hand requires no extra components for modulation and it is, moreover, done without any moving parts.

3. Conclusion

Using the concept of cascaded frequency doubling, we demonstrated a compact diode based laser system emitting 1.9 W of single frequency light at 562.4 nm. Furthermore, we have demonstrated stable operation over a case temperature range of 30K, without actively stabilizing the output power using feedback from a photodiode. By tuning the pump wavelength using the current over the ridge waveguide, we modulated the second harmonic power up to 50 Hz with a modulation depth >90% and a rise time <40 µs. The combination of high stability, compactness and watt-level power range means this technology should be of great interest for a wide range of industries from medical laser treatment to holography.

References

1. S. L. Jacques, "Optical properties of biological tissues: a review," *Phys. Med. Biol.* **58**(11), R37–R61 (2013).
2. V. Kapoor, V. Karpov, C. Linton, F. V. Subach, V. V. Verkhusha, and W. G. Telford, "Solid state yellow and orange lasers for flow cytometry," *Cytom. Part A* **73**(6), 570–577 (2008).

3. W. Telford, M. Murga, T. Hawley, R. Hawley, B. Packard, A. Komoriya, F. Haas, and C. Hubert, "DPSS yellow-green 561-nm lasers for improved fluorochrome detection by flow cytometry," *Cytom. Part A* **68**(1), 36–44 (2005).
4. K. Inagaki, K. Ohkoshi, S. Ohde, G. A. Deshpande, N. Ebihara, and A. Murakami, "Comparative efficacy of pure yellow (577-nm) and 810-nm subthreshold micropulse laser photocoagulation combined with yellow (561-577-nm) direct photocoagulation for diabetic macular edema," *Jpn. J. Ophthalmol.* **59**(1), 21–28 (2015).
5. J. E. Kloepper, T. Bíró, R. Paus, and Z. Cseresnyés, "Point scanning confocal microscopy facilitates 3D human hair follicle imaging in tissue sections," *Exp. Dermatol.* **19**(7), 691–694 (2010).
6. F. V Subach, G. H. Patterson, S. Manley, J. M. Gillette, J. Lippincott-Schwartz, and V. V Verkhusha, "Photoactivatable mCherry for high-resolution two-color fluorescence microscopy.," *Nat. Methods* **6**(2), 153–159 (2009).
7. V. Voliani, G. Signore, O. Vittorio, P. Faraci, S. Luin, J. Peréz-, J. Peréz-Prieto, and F. Beltram, "Cancer phototherapy in living cells by multiphoton release of doxorubicin from gold nanospheres," *J. Mater. Chem. B* **1**(34), 4191–4350 (2013).
8. J. Gao, X. Dai, L. Zhang, H. Sun, and X. Wu, "All-solid-state continuous-wave yellow laser at 561 nm under in-band pumping," *J. Opt. Soc. Am. B* **30**(1), 95 (2012).
9. F. Jia, Q. Zheng, Q. Xue, Y. Bu, and L. Qian, "Yellow light generation by frequency doubling of a diode-pumped Nd:YAG laser," *Opt. Commun.* **259**(1), 212–215 (2006).
10. J. H. Liu, G. C. Sun, and Y. D. Lee, "All-solid-state continuous wave doubly linear resonator sum-frequency mixing yellow laser," *Laser Phys.* **22**(7), 1199–1201 (2012).
11. C. Kränkel, D.-T. Marzahl, F. Moglia, G. Huber, and P. W. Metz, "Out of the blue: semiconductor laser pumped visible rare-earth doped lasers," *Laser Photonics Rev.* **10**(4), 548–568 (2016).
12. P. W. Metz, F. Reichert, F. Moglia, S. Müller, D.-T. Marzahl, C. Kränkel, and G. Huber, "High-power red, orange, and green Pr3+:LiYF4 lasers," *Opt. Lett.* **39**(11), 3193–3196 (2014).
13. P. W. Metz, D.-T. Marzahl, A. Majid, C. Kränkel, and G. Huber, "Efficient continuous wave laser operation of Tb3+-doped fluoride crystals in the green and yellow spectral regions," *Laser Photonics Rev.* **10**(2), 335–344 (2016).
14. E. Kantola, T. Leinonen, S. Ranta, M. Tavast, and M. Guina, "High-efficiency 20 W yellow VECSEL," *Opt. Express* **22**(6), 77–81 (2014).
15. S. Sinha, C. Langrock, M. J. F. Digonnet, M. M. Fejer, and R. L. Byer, "Efficient yellow-light generation by frequency doubling a narrow-linewidth 1150 nm ytterbium fiber oscillator.," *Opt. Lett.* **31**(3), 347–9 (2006).
16. S. Sinha, K. Urbanek, D. Hum, M. J. F. Digonnet, M. M. Fejer, and R. L. Byer, "Linearly polarized, 3.35 W narrow-linewidth, 1150 nm fiber master oscillator power amplifier for frequency doubling to the yellow," *Opt. Lett.* **32**(11), 1530–1532 (2007).
17. M. J. Petrasiunas, M. I. Hussain, J. Canning, M. Stevenson, and D. Kielpinski, "Picosecond 554 nm yellow-green fiber laser source with average power over 1 W," *Opt. Express* **22**(15), 17716 (2014).
18. Y. Feng, L. R. Taylor, and D. B. Calia, "25 W Raman-fiber-amplifier-based 589 nm laser for laser guide star.," *Opt. Express* **17**(21), 19021–19026 (2009).
19. S. Reilly, V. G. Savitski, H. Liu, E. Gu, M. D. Dawson, and A. J. Kemp, "Monolithic diamond Raman laser," *Opt. Lett.* **40**(6), 930–933 (2015).
20. J. I. Kasai, R. Akimoto, T. Hasama, H. Ishikawa, S. Fujisaki, S. Tanaka, and S. Tsuji, "Green-to-yellow continuous-wave operation of BeZnCdSe quantum-well laser diodes at room temperature," *Appl. Phys. Express* **4**(82102), 1–3 (2011).
21. M. A. Majid, A. A. Al-Jabr, R. T. Elafandy, H. M. Oubei, M. S. Alias, B. A. Alnahhas, D. H. Anjum, T. K. Ng, M. Shehata, and B. S. Ooi, "First demonstration of orange-yellow light emitter devices in InGaP/InAlGaP laser structure using strain-induced quantum well intermixing technique," *Proc. SPIE* **9767**, 97670A (2016).
22. K. Paschke, C. Fiebig, G. Blume, F. Bugge, J. Fricke, and G. Erbert, "1120nm highly brilliant laser sources for SHG-modules in bio-analytics and spectroscopy," *Proc. SPIE* **8640**, 86401J–1–8 (2013).
23. K. Paschke, F. Bugge, G. Blume, D. Feise, and G. Erbert, "High-power diode lasers at 1178 nm with high beam quality and narrow spectra.," *Opt. Lett.* **40**(1), 100–2 (2015).
24. J. Hofmann, N. Werner, D. Feise, A. Sahm, R. Bege, B. Eppich, G. Blume, and K. Paschke, "Comparison of yellow light emitting micro integrated laser modules with different geometries of the crystals for second harmonic generation," *Proc. SPIE* **9731**, 973109 (2016).
25. A. Jechow, M. Schedel, S. Stry, J. Sacher, and R. Menzel, "Highly efficient single-pass frequency doubling of a continuous-wave distributed feedback laser diode using a PPLN waveguide crystal at 488 nm.," *Opt. Lett.* **32**(20), 3035–3037 (2007).
26. D. Jedrzejczyk, R. Güther, K. Paschke, B. Eppich, and G. Erbert, "200 mW at 488 nm From a ppMgO:LN Ridge Waveguide by Frequency Doubling of a Laser Diode Module," *IEEE Photonics Technol. Lett.* **22**(17), 1282–1284 (2010).
27. R. Bege, D. Jedrzejczyk, G. Blume, J. Hofmann, D. Feise, K. Paschke, and G. Tränkle, "Watt-level second-harmonic generation at 589 nm with a PPMgO:LN ridge waveguide crystal pumped by a DBR tapered diode laser," *Opt. Lett.* **41**(7), 1530 (2016).
28. D. Jedrzejczyk, R. Güther, K. Paschke, W.-J. Jeong, H.-Y. Lee, and G. Erbert, "Efficient high-power frequency doubling of distributed Bragg reflector tapered laser radiation in a periodically poled MgO-doped lithium niobate planar waveguide.," *Opt. Lett.* **36**(3), 367–369 (2011).
29. A. K. Hansen, M. Tawfieq, O. B. Jensen, P. E. Andersen, B. Sumpf, G. Erbert, and P. M. Petersen, "Concept for power scaling second harmonic generation using a cascade of nonlinear crystals," *Opt. Express* **23**(12), 15921 (2015).
30. Y. H. Kwon, D. K. Lee, and O. W. Kwon, "The Short-term Efficacy of Subthreshold Micropulse Yellow (577-nm) Laser Photocoagulation for Diabetic Macular Edema," *Korean J. Ophthalmol.* **28**(5), 379 (2014).